Zeros of the Spectrogram of White Noise with Hermite Windows

Charaf Bellourak[a], Sylvain Meignen[a], Kévin Polisano[a], Mickaël Nahon[a]

[a] *Jean Kuntzmann Laboratory, University Grenoble Alpes and CNRS 5225, Grenoble 38401, France*

Abstract

We study the zeros of the spectrogram of complex white noise analyzed with Hermite windows of order n, extending the classical Gaussian-window correspondence with Gaussian Analytic Functions to the polyanalytic setting. Using the polyanalytic Bargmann transform, these zeros split into two families according to the sign of the local Jacobian, giving rise to a natural notion of charge, and we show that these zeros are almost surely simple, isolated, and form a translation and rotation-invariant point process. We derive closed-form expressions for the one-point intensity, decomposed by charge, and also for the unsigned, signed, and hybrid two-point intensities. Besides, we prove that unlike the total repulsion observed with a Gaussian window, the Hermite window of order n generates a pair correlation function that converges at the origin to a strictly positive constant depending on n. Finally, we propose a numerical method for detecting spectrogram zeros via the winding number around candidate local minima.

Keywords: Short-time Fourier transform, white noise spectrograms, Hermite polynomials, polyanalytic functions, Kac-Rice formulas, pair-correlations, winding number.

1. Introduction

The time-frequency analysis of white noise has seen significant development in recent years, particularly through the establishment of deep connections between the short-time Fourier transform (STFT) and the theory of Gaussian analytic random functions. This line of research originates in the pioneering empirical observations of Flandrin [1], who noticed that the zeros of the spectrogram of white Gaussian noise, computed with a Gaussian window, are distributed according to a regular pattern and proposed a filtering method based on the Delaunay triangulation of these zeros. Then a rigorous mathematical framework was proposed independently by [2] and [3], who both established that when the analysis window used is the unitary Gaussian functions, the spectrogram of complex white noise gives rise to a point process whose zeros coincide with those of a well-known Gaussian Analytic Function (GAF) associated with

the Bargmann-Fock space, an object whose statistical structure (rotation invariance, zero repulsion, pair correlation function) has been extensively studied in the probabilistic literature, notably by Hough [4]. This identification provided a rigorous explanation for Flandrin's empirical observations and a solid probabilistic foundation for characterizing the zeros distribution.

Bardenet and Hardy [5] later developed a systematic correspondence between pairs (time-frequency transform, GAF) and generating functions of classical orthogonal polynomials, also extending this unifying framework to the wavelet transform and its associated hyperbolic GAF. In parallel, [3] extended the zero-based filtering technique to the continuous wavelet transform and provided statistical tools like pair correlation estimators for the design of such algorithms.

However, all of theses works restrict their attention to windows leading to genuinely holomorphic random functions. This restriction naturally raises the question of its generalization: what happens when the Gaussian window is replaced by a Hermite window of order $n \geq 1$? Indeed this natural choice has been motivated in particular by the multitaper and reassignment methods discussed by Flandrin [6] and by the ConceFT algorithm of Daubechies et al. [7] which combines several Hermite windows to sharpen time-frequency representations. Hermite functions have also been studied as windows for Gabor frames and superframes [8, 9], with recent work focusing on asymptotic frame regions associated with high-order Hermite functions [10]. As shown by Abreu and Shirai in a recent work [11], replacing the Gaussian window by a Hermite window h_n of order n has the effect of replacing classical GAF by a polyanalytic random functions. This work reveals a correlation structure between the zero sets of spectrograms associated with different Hermite orders, providing a rationale for the empirically observed efficiency of multitaper techniques. Nevertheless, this polyanalytic setting has so far received comparatively little attention from the point of view of intrinsic statistics of the zeros of a single spectrogram with h_n, as opposed to the cross-correlations between different orders n.

The goal of this article is twofold, and complement this recent work by focusing on the single-window case. First, we establish the theoretical framework necessary to study the zeros of the spectrogram obtained with a Hermite window of order n, relying on the Bargmann transform and complex Hermite polynomials. In particular, we show that these zeros, unlike in the classical holomorphic case treated in these earlier works, split into two families according to the sign of the Jacobian of the associated polyanalytic function, giving rise to a notion of charge of the zeros, either positive or negative [12]. Second, we develop the statistical tools needed to characterize this new point process: we compute the signed and unsigned pair correlation functions, and we derive the asymptotic behavior of the pair correlation function near the origin. Finally, motivated by practical considerations regarding the numerical detection of zeros in a spectrogram, we propose and analyze a detection method based on computing the winding number around local minima of the spectrogram, and we discuss the optimal choice of the contour radius used for this detection.

The remainder of the article is organized as follows. Section 2 recalls basic notions on the STFT, the Bargmann transform, and polyanalytic Fock spaces.

Section 3 gives the polyharmonic Bargmann transform of white Gaussian noise and some stationarity properties. Section 4 establishes the fundamental properties of the zeros of the white noise spectrogram with Hermite windows, in particular their characterization in terms of charge. Section 5 is devoted to the computation of the pair correlation function and the study of its asymptotic behavior. Section 6 proposes a numerical method for zero detection and discusses the choice of the optimal contour radius. Technical proofs are deferred to the appendix.

2. Background

2.1. The Short-Time Fourier Transform

Let $f, g \in L^2(\mathbb{R})$, the evaluation at $(u, v) \in \mathbb{R}^2$ of the *short-time Fourier transform* (STFT) of f with window g reads

$$V_g f(u,v) = \int_{\mathbb{R}} f(t)\, \overline{g(t-u)}\, e^{-2i\pi vt}\, dt = \langle f, M_v T_u g \rangle, \tag{1}$$

with $\langle \cdot, \cdot \rangle$ the inner product in $L^2(\mathbb{R})$, $M_v f = e^{2i\pi v \cdot} f(\cdot)$, and $T_u f = f(\cdot - u)$. The squared modulus of the STFT, $|V_g f(u,v)|^2$, is called the *spectrogram*. The right-hand side of (1) naturally extends the STFT to tempered distributions [13], which will be relevant later for white noise. For a fixed window $g \in L^2(\mathbb{R})$, the STFT maps $L^2(\mathbb{R})$ to a closed subspace of $L^2(\mathbb{R}^2)$, noted $\mathcal{G}_g$, called the *Gabor space*:

$$\mathcal{G}_g = \left\{ V_g f : f \in L^2(\mathbb{R}) \right\} \subset L^2(\mathbb{R}^2). \tag{2}$$

If $\|g\|_{L^2(\mathbb{R})} = 1$, then V_g is an isometry from $L^2(\mathbb{R})$ onto $\mathcal{G}_g$. In what follows we denote by $\langle \cdot, \cdot \rangle_2$ on $L^2(\mathbb{R}^2)$. Hence $\mathcal{G}_g$ is a reproducing kernel Hilbert space with kernel

$$k(u,v,u',v') = \langle M_v T_u g,\, M_{v'} T_{u'} g \rangle_2. \tag{3}$$

In what follows, g denotes $g(x) = 2^{1/4} e^{-\pi x^2}$ unless stated otherwise. Using that function, writing $z = u + iv$ and $w = u' + iv'$, this kernel $k_0(z, w)$ is given by [14]:

$$k_0(z,w) = e^{-i\pi(u'v' - uv) - \frac{\pi}{2}(|z|^2 + |w|^2)}\, e^{\pi w \bar{z}}. \tag{4}$$

2.2. The Bargmann Transform and Fock Space

Recall that $\mathcal{L}^2(\mathbb{C}) := L^2(\mathbb{C}, e^{-\pi|z|^2})$ denotes the Hilbert space of all measurable functions $F : \mathbb{C} \to \mathbb{C}$ equipped with the norm

$$\|F\|^2_{\mathcal{L}^2(\mathbb{C})} = \int_{\mathbb{C}} |F(z)|^2 e^{-\pi|z|^2}\, d\mu(z) < \infty,$$

where $\mu(z)$ is the Lebesgue measure on $\mathbb{C}$. For the unitary Gaussian window g, the STFT admits the classical Bargmann representation [15]:

$$V_g f(\bar{z}) := V_g f(u, -v) = e^{\pi i u v} e^{-\frac{\pi}{2}|z|^2} \mathcal{B} f(z), \tag{5}$$

where $\mathcal{B}f$ is the Bargmann transform defined by:

$$\mathcal{B}f(z) = 2^{1/4} \int_{\mathbb{R}} f(t)\, e^{-\pi t^2 + 2\pi t z - \frac{\pi}{2} z^2}\, dt. \tag{6}$$

This identifies the STFT as an entire function of z. More precisely, the Bargmann transform maps $L^2(\mathbb{R})$ isometrically onto the Fock space $\mathcal{F}(\mathbb{C})$ [16], defined as the Hilbert space of entire functions F of $L^2(\mathbb{C}, e^{-\pi|z|^2})$. In what follows we denote $\langle \cdot, \cdot \rangle_{\mathcal{F}}$ the inner product on $\mathcal{F}(\mathbb{C})$. This space is a reproducing kernel Hilbert space with kernel

$$K^0(z, w) = e^{\pi z \bar{w}}. \tag{7}$$

Remark 2.1. *Using (5) and (7), one easily obtains (4).*

2.3. Gabor space, Hermite functions and polyanalytic functions

Let us consider the family of Hermite functions $(h_n)_{n \geq 0}$, defined by:

$$h_n(t) = (-1)^n \frac{2^{1/4}}{\sqrt{2^n n!}} e^{\pi t^2} \frac{d^n}{dt^n} e^{-2\pi t^2}. \tag{8}$$

Definition 2.1. *The corresponding Gabor space $\mathcal{G}^n$ is:*

$$\mathcal{G}^n = \left\{ V_{h_n} f : f \in L^2(\mathbb{R}) \right\} \subset L^2(\mathbb{R}^2). \tag{9}$$

The kernel of $\mathcal{G}^n$ is given in [14]:

$$k_n(z, w) = \frac{1}{n!}\, e^{i\pi(uv - u'v') + \frac{\pi}{2}(|w|^2 - |z|^2)} \left(\frac{d}{dw} \right)^n \left[e^{\pi \bar{z} w - \pi |w|^2} (w - z)^n \right]. \tag{10}$$

Definition 2.2 (Polyanalytic function)**.** *A function $F : \mathbb{C} \to \mathbb{C}$ is called* Polyanalytic *of order n if its $(n+1)$-th derivative with respect to $\bar{z}$ vanishes, that is,*

$$\partial_{\bar{z}}^{n+1} F = 0. \tag{11}$$

Equivalently, F can be written as:

$$F(z) = \sum_{k=0}^{n} \bar{z}^k \phi_k(z), \tag{12}$$

where $\{\phi_k\}_{k=0}^n$ are analytic functions.

Definition 2.3 (The true polyanalytic Fock space)**.** *A function $F : \mathbb{C} \to \mathbb{C}$ belongs to the* True Polyanalytic Fock space $\mathcal{F}^n(\mathbb{C})$ *of order n if $\|F\|^2_{\mathcal{L}^2(\mathbb{C})} < \infty$*

and there exists an entire function ϕ such that:

$$F(z) = \left(\frac{\pi^n}{n!}\right)^{\frac{1}{2}} \; e^{\pi|z|^2} \left(\frac{d}{dz}\right)^n \left(e^{-\pi|z|^2}\phi(z)\right). \tag{13}$$

Remark 2.2. 1. *$n = 0$ corresponds to analytic functions.*
2. *Every function of $\mathcal{F}^n(\mathbb{C})$ is polyanalytic of order n.*

Definition 2.4. *The true polyanalytic Bargmann transform of order n of a function $f \in L^2(\mathbb{R})$ is defined by:*

$$(\mathcal{B}_n f)(z) = \left(\frac{\pi^n}{n!}\right)^{\frac{1}{2}} \; e^{\pi|z|^2} \left(\frac{d}{dz}\right)^n \left(e^{-\pi|z|^2}\mathcal{B}f\right)(z). \tag{14}$$

Using (13) and the fact that $\mathcal{B}f$ is an entire function, it is clear that $\mathcal{B}_n f$ ($n \geq 1$) is a polyanalytic function. The STFT computed with h_n and the polyanalytic Bargmann transform are related through:

$$(\mathcal{B}_n f)(z) = e^{-i\pi uv + \frac{\pi}{2}|z|^2} \, (V_{h_n} f)(u, -v), \tag{15}$$

which defines a mapping between $L^2(\mathbb{R})$ and $\mathcal{F}^n(\mathbb{C})$ [14, 17].

The multiplier operator

$$(\mathcal{E}_n F)(z) = e^{i\pi uv + \frac{\pi}{2}|z|^2} F(z) \tag{16}$$

defines an isometric isomorphism $\mathcal{G}^n \cong \mathcal{F}^n(\mathbb{C})$.

Proposition 2.1. *The space $\mathcal{F}^n(\mathbb{C})$ is a reproducing kernel Hilbert space and its kernel $K^n(z, w)$ is the following:*

$$K^n(z, w) = e^{-i\pi(uv - u'v') + \frac{\pi}{2}(|w|^2 + |z|^2)} k_n(z, w). \tag{17}$$

Proof. Let $f \in \mathcal{G}^n$ and $\psi = \mathcal{E}_n f \in \mathcal{F}^n(\mathbb{C})$, the reproducing property gives $f(z) = \langle f, k_n(z, \cdot)\rangle_{\mathcal{G}^n}$. As $\mathcal{E}_n$ is unitary,

$$\langle f, k_n(z, \cdot)\rangle_2 = \quad \langle \mathcal{E}_n f, \mathcal{E}_n k_n(z, \cdot)\rangle_{\mathcal{F}} = \langle \psi, \mathcal{E}_n k_n(z, \cdot)\rangle_{\mathcal{F}}.$$

Then, $e^{-i\pi uv - \frac{\pi}{2}|z|^2}\psi(z) = \langle \psi, e^{i\pi u'v' + \frac{\pi}{2}|w|^2} k_n(z, \cdot)\rangle_{\mathcal{F}}$ meaning that

$$\psi(z) = \langle \psi, K_n(z, \cdot)\rangle_{\mathcal{F}_n(\mathbb{C})}.$$

□

Combining (17) with (10), one obtains:

$$K^n(z, w) = \frac{1}{n!} \, e^{\pi|w|^2} \left(\frac{d}{dw}\right)^n \left[e^{\pi\bar{z}w - \pi|w|^2}(w - z)^n\right] = L_n(\pi|z - w|^2) \, e^{\pi w\bar{z}}, \tag{18}$$

where L_n is the Laguerre polynomial of degree n.

Finally, we prove the following proposition:

Proposition 2.2. *The* STFT *of an Hermite function h_k with the window h_n is given by:*

$$V_{h_n} h_k(\bar{z}) = e^{i\pi uv} e^{-\frac{\pi}{2}|z|^2} H_{k,n}(\sqrt{\pi}\ z, \sqrt{\pi}\ \bar{z}), \tag{19}$$

where $H_{k,n}$ stands for the complex Hermite polynomials defined as [11]:

$$H_{k,n}(z,\bar{z}) = \begin{cases} \sqrt{\dfrac{n!}{k!}}\, z^{k-n} L_n^{(k-n)}\big(|z|^2\big), k > n, \\ \sqrt{\dfrac{k!}{n!}}\, (-\bar{z})^{\,n-k} L_k^{(n-k)}\big(|z|^2\big), k \leq n, \end{cases}$$

with $L_n^{(\alpha)}$ the generalized Laguerre polynomial.

The proof is available in Appendix 8.1.

3. Polyharmonic Bargmann transform of white Gaussian noise and stationarity properties

3.1. Polyharmonic Bargmann transform of white Gaussian noise

A *complex Gaussian white noise* (CGWN) can be viewed as a random tempered distribution, denoted by $\mathcal{S}'(\mathbb{R})$, and its Hermite coefficients are i.i.d. standard complex Gaussian random variables [11]. More precisely, since $(h_k)_{k\geq 0}$ is an orthonormal basis of $L^2(\mathbb{R})$, then the decomposition of white noise into this basis can be written in $\mathcal{S}'(\mathbb{R})$ as

$$\xi = \sum_{k=0}^{\infty} \xi_k h_k, \tag{20}$$

where the random variables $\xi_k := \langle \xi, h_k \rangle$ are i.i.d. with law $\mathcal{CN}(0,1)$. As the convergence takes place in $\mathcal{S}'(\mathbb{R})$, we may write:

$$\begin{aligned} V_{h_n}\xi\left(\frac{\bar{z}}{\sqrt{\pi}}\right) &= \langle \xi, M_{-v}T_u h_n\rangle = \sum_{k=0}^{\infty} \xi_k V_{h_n} h_k\left(\frac{\bar{z}}{\sqrt{\pi}}\right) \\ &= e^{iuv} e^{-\frac{|z|^2}{2}} \sum_{k=0}^{\infty} \xi_k H_{k,n}(z,\ \bar{z}) := e^{iuv} e^{-\frac{|z|^2}{2}} f_n(z,\bar{z}). \end{aligned} \tag{21}$$

So using (15), we have $(\mathcal{B}_n\xi)(\frac{z}{\sqrt{\pi}}) = f_n(z,\bar{z})$. One also has the following relation [11]:

$$f_{n+1}(z,\bar{z}) = \frac{1}{\sqrt{n+1}}(\partial_z f_n(z,\bar{z}) - \bar{z} f_n(z,\bar{z})). \tag{22}$$

For the sake of simplicity, from now on we will put $f_n(z) := f_n(z,\bar{z})$.

3.2. Stationarity with respect to translation

Consider the kernel associated with $\mathcal{B}_n(z+a)$, we immediately get:

$$K^n(z+a,w+a) \quad = \quad L_n(\pi|z-w|^2)\, e^{\pi(w+a)\overline{z+a}} = K^n(z,w)\, e^{\pi(a\bar{z}+w\bar{a}+|a|^2)}.$$

Defining $h_n(z) := \mathcal{B}_n(z)e^{\pi(z\bar{a}+\frac{|a|^2}{2})}$, one gets:

$$\mathbb{E}[h_n(w)\overline{h_n(z)}] = K^n(z,w)\, e^{\pi(a\bar{z}+w\bar{a}+|a|^2)}.$$

Thus we have

$$\mathcal{B}_n(z+a) := e^{\pi(z\bar{a}+\frac{|a|^2}{2})}\mathcal{B}_n(z). \tag{23}$$

The prefactor of the right-hand side is nonzero, thus the zeros of $\mathcal{B}_n(z)$ are invariant with respect to translation.

3.3. Stationarity with respect to rotation

Remembering that

$$f_n(z,\bar{z}) = \sum_{k=0}^{n} \binom{n}{k} f_0^{(k)}(z)(-\bar{z})^{n-k}.$$

Thus,

$$\begin{aligned} f_n(e^{i\theta}z, e^{-i\theta}\bar{z}) &= \sum_{k=0}^{n} \binom{n}{k} f_0^{(k)}(e^{i\theta}z)(-e^{-i\theta}\bar{z})^{n-k} \\ &= \sum_{k=0}^{n} \binom{n}{k} \sum_{p\geq k} \xi_p \frac{\sqrt{p!}}{(p-k)!} z^{p-k} e^{i\theta(p-k)} (-e^{-i\theta}\bar{z})^{n-k} \\ &= \sum_{k=0}^{n} \binom{n}{k} \sum_{p\geq k} \xi_p e^{i\theta(p-n)} \frac{\sqrt{p!}}{(p-k)!} z^{p-k} (\bar{z})^{n-k}, \end{aligned}$$

therefore $f_n(e^{i\theta}z) \overset{d}{=} f_n(z)$.

4. Zeros of White Noise with Hermite Functions

4.1. Zeros of White Noise as a Point Process

The polyanalytic function f_n has the same zeros as $V_{h_n}\xi$, thus we study the zeros of the former function. We already know that when $n = 0$, the zeros are isolated [5]. Then using (22), one can write that if $n = 0$ the zeros z_0 of f_1 correspond to:

$$\partial_z f_0(z_0) - \bar{z}_0 f_0(z_0) = 0.$$

Now assume that $f_0(z_0) \neq 0$, then f_0 is holomorphic at z_0 and we may write:

$$\bar{z}_0 := A(z_0) = \frac{\partial_z f_0(z_0)}{f_0(z_0)},$$

with A holomorphic at z_0 at thus defining $\overline{A}$, the conjugate of A, we may write $z_0 = \overline{A}(\bar{z}_0) = \overline{A} \circ A(z_0)$. Then, as $\overline{A} \circ A$ is holomorphic at z_0, then z_0 is a fixed point of an holomorphic function and is isolated provided $\overline{A} \circ A$ is not the identity, which is true with probability 1. Then if $f_0(z_0) = 0$ then $\partial_z f_0(z_0) = 0$ and thus z_0 is a second order zero of an holomorphic function and is therefore isolated.

In the general case, $n \geq 1$, let us consider $f_n(z, \bar{z}) = u(z, \bar{z}) + iv(z, \bar{z})$, then the zeros correspond to $f_n(z_0, \bar{z}_0) = 0$ and, omitting $(z_0, \bar{z}_0)$ for the sake of simplicity:

$$\det f_n'(z_0) = \begin{vmatrix} \partial_x u & \partial_y u \\ \partial_x v & \partial_y v \end{vmatrix} = |\partial_z f_n|^2 - |\partial_{\bar{z}} f_n|^2 = 0. \tag{24}$$

So viewing $f_n(z, \bar{z})$ as a bidimensional function, it is clear that when (24) is satisfied, there may exist a curve of zeros around $z = z_0$, and z_0 is called a degenerate zero. On the contrary, when (24) is not satisfied, the zeros are isolated.

The Bulinskaya-type lemma implies that, for the random field f_n, degenerate zeros occur with probability zero, therefore the zeros are almost surely isolated and simple even for $n \geq 1$. For the sake of consistency we recall [11, 18]:

Lemma 4.1 (Bulinskaya-type lemma)**.** *Let $U \subset \mathbb{R}^2$ be open, and let $F : U \to \mathbb{R}^2$ be a random field with almost surely C^1 sample paths. Fix $v \in \mathbb{R}^2$. Assume that for every relatively compact open set $O \subset U$, there exists a neighborhood V of v and a constant C_O such that for every $y \in V$,*

$$\int_O p_{F(x)}(y)\, dx \leq C_O, \tag{25}$$

where $p_{F(x)}$ denotes the density of $F(x)$ on $\mathbb{R}^2$. Then

$$\mathbb{P}\Big(\exists\, x \in O : F(x) = v \text{ and } \det F'(x) = 0\Big) = 0. \tag{26}$$

In other words, with probability one, the level v is not a critical value of F.

A direct application of this lemma consists of considering the random field $F_n(z) = \big(\Re f_n(z, \bar{z}),\, \Im f_n(z, \bar{z})\big) \in \mathbb{R}^2$, which is almost surely C^1 for each noise realization and admits a density $p_{F_n(z)}$ on $\mathbb{R}^2$ satisfying

$$\int_O p_{F(z)}(y)\, dz \leq \frac{|O|}{\pi}$$

for every relatively compact set $O \subset \mathbb{C}$ and every $y \in \mathbb{R}^2$ (see [11, Proposition

4.8]).

Therefore the assumptions of the lemma are satisfied and, taking $v = 0$, one concludes that the zeros of $f_n(z, \bar{z})$ are almost surely simple and isolated, and thus define a point process, which can be studied using statistical tools like *pair correlation function*.

When $n \geq 1$, there exists three types of zeros depending on the sign of the Jacobian of f_n defined by

$$J_{f_n}(z_0) = |\partial_z f_n(z_0)|^2 - |\partial_{\bar{z}} f_n(z_0)|^2. \tag{27}$$

If $J_{f_n}(z_0) > 0$ (resp. < 0), we say that the zero is charged positively (resp. negatively). When it is null, the zero is said to be degenerate, a situation that happens with a null probability since the zeros are point processes.

4.2. On Maxima and Zeros of $|V_{h_0}\xi|^2$ and $|V_{h_1}\xi|^2$

We investigate the relation between maxima at order 0 and zeros at order 1. If z_0 is a zero of f_1, considering ϕ_0 defined as:

$$\phi_0(z) := |f_0(z)|^2 e^{-|z|^2}. \tag{28}$$

A direct computation, using the fact f_0 is holomorphic, gives:

$$\partial_z \phi_0(z) = f_1(z)\,\overline{f_0(z)} e^{-|z|^2}. \tag{29}$$

Therefore, the critical points of ϕ are exactly the points where $f_0(z) = 0$ or $f_1(z) = 0$. $f_0(z) = 0$ obviously corresponds to minima of ϕ_0. To determine whether critical points corresponding to $f_1(z) = 0$ are maxima or saddle points, we look into the Hessian matrix $H(z)$ of $\phi_0(z)$. In fact, we have the following:

- If $\det H(z) > 0$ and $\partial_z \partial_{\bar{z}} \phi_0(z) < 0$, then there is a local maxima at z.
- If $\det H(z) < 0$, then there is a saddle point at z.

Using (29), we get:

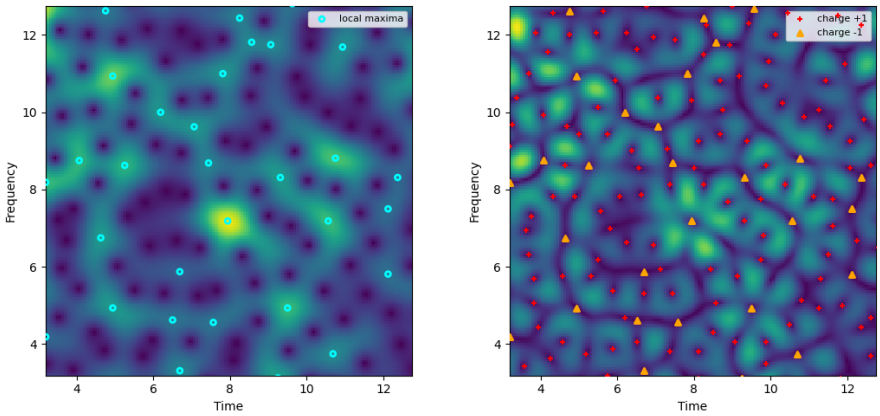
$$\begin{aligned}\partial_z \partial_{\bar{z}} \phi_0(z) &= e^{-|z|^2}\Big(|f_1(z)|^2 + f_0(z)\overline{\partial_{\bar{z}} f_1(z)}\Big) \\ &= e^{-|z|^2}\Big(|f_1(z)|^2 - |f_0(z)|^2\Big) = -e^{-|z_0|^2}\ |f_0(z_0)|^2 < 0,\end{aligned}$$

in which we used the fact that f_0 is holomorphic to write $\partial_{\bar{z}} f_1 = -f_0$. For the determinant of the Hessian matrix, one has

$$\det H(z) = 4\Big[(\partial_z \partial_{\bar{z}} \phi_0(z))^2 - |\partial_z^2 \phi_0(z)|^2\Big]. \tag{30}$$

We then remark that

$$\partial_z^2 \phi_0(z) = e^{-|z|^2}\ \overline{f_0(z)}\ \big(\partial_z f_1(z) - \bar{z}\, f_1(z)\big).$$



(a) (b)

Figure 1: (a): local maxima of $|V_{h_0}\xi|^2$. (b): positive and negative zeros of $|V_{h_1}\xi|^2$

Now consider z_0 such that $f_1(z_0) = 0$ and $f_0(z_0) \neq 0$, one obtains

$$\partial_z^2 \phi_0(z_0) = e^{-|z_0|^2}\, \overline{f_0(z_0)}\, \partial_z f_1(z_0),$$

and thus (30) becomes

$$\begin{aligned} \det H(z_0) =& 4e^{-2|z_0|^2}|f_0(z_0)|^2\Big(|f_0(z_0)|^2 - |\partial_z f_1(z_0)|^2\Big) \\ =& 4e^{-2|z_0|^2}|f_0(z_0)|^2\Big(|\partial_{\bar z} f_1(z_0)|^2 - |\partial_z f_1(z_0)|^2\Big) \\ =& -4e^{-2|z_0|^2}|f_0(z_0)|^2\ J_{f_1}(z_0), \end{aligned} \tag{31}$$

and thus the local maxima (resp. saddle points) of $|V_{h_0}\xi|^2$ are the zeros of f_1 charged negatively (resp. positively) as illustrated in Fig. 1. Unfortunately, there is no extension to $n \geq 1$, because f_n is no longer holomorphic.

5. Computation of the one and two points intensities

Using Kac-Rice Formula, the k-point intensity of f_n is defined as follows:

$$\begin{aligned} &\rho_n^{[k]}(a_1, a_2, \dots, a_k) = \\ &\mathbb{E}[|J_{f_n(a_1)} \dots J_{f_n(a_k)}| \mid f_n(a_1) = 0, \dots, f_n(a_k) = 0] p_{f_n(a_1),\dots,f_n(a_k)}(0, \dots, 0). \end{aligned} \tag{32}$$

As f_n is stationary, we had rather study its simpler form, setting a_1 to zero:

$$\begin{aligned} &\rho_n^{[k]}(0, a_2, \dots, a_k) = \\ &\mathbb{E}[|J_{f_n(0)} \dots J_{f_n(a_k)}| \mid f_n(0) = 0, \dots, f_n(a_k) = 0] p_{f_n(0),\dots,f_n(a_k)}(0, \dots, 0). \end{aligned} \tag{33}$$

So if $k=1$, we obtain the 1-point intensity which is constant, and multiplied by π we get the average number of zero on circles of radius 1 on $|V_{h_n}\xi|^2$. If $k=2$, and multiplying by π (see normalization in (21)), $\rho_n^{[2]}$ is related to the probability of having 2 zeros of $|V_{h_n}\xi|^2$ in a discus of radius r in the complex plane.

5.1. Computation of the First Intensity of Hermite Zeros

Though a proof of the calculation of the 1-point intensity already exists in [12, Theorem 1.8]. We propose here a much simpler version, based on a different approach. To compute the 1-point intensity we recall that

$$\begin{aligned} f_0(z) &= \sum_k \xi_k \frac{z^k}{\sqrt{k!}}, \\ f_n(z) &= \frac{1}{\sqrt{n!}}(\partial_z - \bar{z})^n f_0(z) = \frac{1}{\sqrt{n!}} \sum_{k=0}^{n} \binom{n}{k} f_0^{(k)}(z)(-\bar{z})^{n-k}. \end{aligned}$$

Then the Jacobian of $f_n(z)$ reads $J_{f_n}(z) = |\partial_z f_n(z)|^2 - |\partial_{\bar{z}} f_n(z)|^2$. Because of the stationarity of the process f_n with respect to translation (see Sec. 3.2), one can compute the 1-point intensity using Kac-Rice formula at zero. We first remark that:

$$J_{f_n}(0) = \left| \frac{f_0^{(n+1)}(0)}{\sqrt{n!}} \right|^2 - \left| n \frac{f_0^{(n-1)}(0)}{\sqrt{n!}} \right|^2 = (n+1)|\xi_{n+1}|^2 - n|\xi_{n-1}|^2,$$

and then that

$$p_{f_n(z)}(y) = \frac{1}{\pi K^n\left(\frac{z}{\sqrt{\pi}}, \frac{z}{\sqrt{\pi}}\right)} e^{-\frac{|y|^2}{K^n\left(\frac{z}{\sqrt{\pi}}, \frac{z}{\sqrt{\pi}}\right)}},$$

we obtain using the Kac-Rice formula that:

$$\rho_n^{[1]} = \mathbb{E}[|J_{f_n}(0)| \ | f_n(0) = 0] p_{f_n(0)}(0) = \frac{\mathbb{E}[|J_{f_n}(0)| \ | f_n(0) = 0]}{\pi}. \tag{34}$$

Then, we remark that $f_n(0) = \frac{f_0^{(n)}(0)}{\sqrt{n!}} = \xi_n$. Thus, $J_{f_n}(0)$ is independent from $f_n(0)$. Consequently:

$$\rho_n^{[1]} = \frac{\mathbb{E}[|J_{f_n}(0)|]}{\pi} = \frac{\mathbb{E}[|(n+1)|\xi_{n+1}|^2 - n|\xi_{n-1}|^2|]}{\pi}$$

$$= \frac{1}{\pi}\left\{(n+1)\mathbb{E}[|\xi_{n+1}|^2] + n\mathbb{E}[|\xi_{n-1}|^2] - 2\mathbb{E}[\min((n+1)|\xi_{n+1}|^2, n|\xi_{n-1}|^2)]\right\}.$$

Using the fact that, for any n, ξ_n is $\mathcal{CN}(0,1)$, its real and imaginary parts are $\mathcal{N}(0,\frac{1}{2})$, and thus $2|\xi_n|^2$ is χ_2 distributed with 2 degrees of freedom and thus $\mathbb{E}[|\xi_n|^2] = \mathbb{E}[|\xi_{n+1}|^2] = 1$. Then, using properties on the expectation of the minimum of weighted χ_2 laws, we may write:

$$\mathbb{E}[\min((n+1)|\xi_{n+1}|^2, n|\xi_{n-1}|^2)] = \frac{(n+1)n}{2n+1}.$$

Putting everything together we obtain:

$$\rho_n^{[1]} \quad = \quad \frac{1}{\pi}\left(n+\frac{1}{2}+\frac{1}{4n+2}\right). \tag{35}$$

Let us then derive the 1-point intensities of the positive and negative charges. In what follows, we denote $\rho_n^{[1],+}$ (resp. $\rho_n^{[1],-}$), the 1-point intensity of the zeros charged positively (resp. negatively), namely $f_n(z_0) = 0$ with $J_{f_n}(z_0) > 0$ (resp. $J_{f_n}(z_0) < 0$). For that we use (34) but with the signed Jacobian:

$$\rho_n^{[1],+} - \rho_n^{[1],-} = \frac{\mathbb{E}[J_{f_n}(0) \mid f_n(0) = 0]}{\pi n!} = \frac{\mathbb{E}[(n+1)|\xi_{n+1}|^2 - n|\xi_{n-1}|^2]}{\pi} = \frac{1}{\pi}. \tag{36}$$

Using the fact that:

$$\rho_n^{[1],+} + \rho_n^{[1],-} \quad = \quad \rho_n^{[1]},$$

the 1-point intensities of positive and negative charges are given respectively by:

$$\rho_n^{[1],+} = \frac{1}{2\pi}\left(n+\frac{3}{2}+\frac{1}{4n+2}\right),\ \rho_n^{[1],-} = \frac{1}{2\pi}\left(n-\frac{1}{2}+\frac{1}{4n+2}\right).$$

5.2. Computation of the 2-point intensity of Hermite zeros

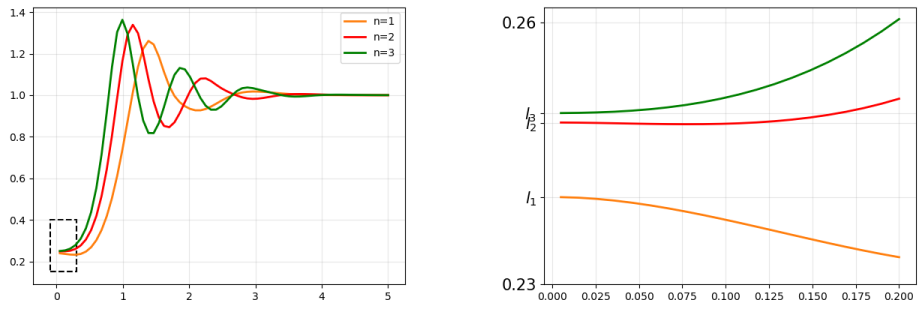
The 2-points intensity of f_n satisfies the following property:

$$\begin{aligned}
\rho_n^{[2]}(0,a_2) &= \mathbb{E}[|J_{f_n(0)}J_{f_n(a_2)}| \mid f_n(0) = f_n(a_2) = 0]p_{f_n(0),f_n(a_2)}(0,0) \\
&= \mathbb{E}[|J_{f_n(0)}J_{f_n(e^{-i\theta_2}a_2),}| \mid f_n(0) = f_n(e^{-i\theta_2}a_2) = 0]p_{f_n(0),f_n(e^{-i\theta_2}a_2)}(0,0) \\
&= \mathbb{E}[|J_{f_n(0)}J_{f_n(r)}| \mid f_n(0) = f_n(r) = 0]p_{f_n(0),f_n(r)}(0,0) = \rho_n^{[2]}(0,|a_2|).
\end{aligned}$$

We therefore put $\rho_n^{[2]}(r)$ for $r \in \mathbb{R}_*^+$ (r can be viewed as $|a_2|$). We first define

$$X = \begin{pmatrix} f_n(0) \\ f_n(r) \end{pmatrix},\ Y = \begin{pmatrix} \partial_z f_n(0) \\ \partial_{\bar{z}} f_n(0) \\ \partial_z f_n(r) \\ \partial_{\bar{z}} f_n(r) \end{pmatrix}. \tag{37}$$

Both X and Y are zero mean Gaussian vectors. In that case, $Z = (Y \mid X = 0)$ follows a Gaussian law with expectation vector and covariance matrix defined



(a) (b)

Figure 2: (a): $g_n^{[2]}(r)$ for $n = 1, 2$ and 3 (b): Zoom of the dashed black square, highlighting l_1, l_2 and l_3.

by:

$$\begin{aligned} \mathbb{E}[Z] = \mathbb{E}[Y] = 0_{\mathbb{R}^4}, \\ \Gamma = \Sigma_Y - (\Sigma_0)^H (\Sigma_X)^{-1} \Sigma_0, \end{aligned} \tag{38}$$

with $\Sigma_Y = \mathrm{Cov}(Y)$, $\Sigma_X = \mathrm{Cov}(X)$, $\Sigma_0 = \mathrm{Cov}(X, Y)$, and, H denotes the Hermitian transpose. To compute the 2-point intensity we also need:

$$p_{f_n(0), f_n(r)}(y) = \frac{1}{\pi^2 \det \Sigma_X} e^{-y^* (\Sigma_X)^{-1} y}. \tag{39}$$

Then, let $\tilde{Z}$ be a centered complex Gaussian vector in $\mathbb{C}^d$ with covariance matrix $\Gamma \succeq 0$, and let $A \in \mathcal{M}_d(\mathbb{C})$ be Hermitian. Then for every $t \in \mathbb{R}$ [19],

$$\mathbb{E}\left[\exp(it\tilde{Z}^* A \tilde{Z})\right] = \det(I - it\Gamma A)^{-1}. \tag{40}$$

Let us now apply this result to the centered complex Gaussian vector Z with covariance $\Gamma \succeq 0$ and the hermitian matrix Λ, defined by

$$\Lambda(s, t) = sA_1 + tA_2,$$

with $A_1 = \mathrm{Diag}(1, -1, 0, 0)$ and $A_2 = \mathrm{Diag}(0, 0, 1, -1)$, and $s, t \in \mathbb{R}$. Then we introduce

$$J_0 := Z^* A_1 Z, \; J_r := Z^* A_2 Z.$$

With these notations we can express the 2-point intensity as

$$\rho_n^{[2]}(r) := \mathbb{E}[|J_{f_n(0)} J_{f_n(r)}| \mid f_n(0) = f_n(r) = 0] p_{f_n(0), f_n(r)}(0, 0) = \frac{\mathbb{E}[|J_0 J_r|]}{\pi^2 \det \Sigma_X}. \tag{41}$$

Then defining the function φ as:

$$\begin{aligned}\varphi(s,t) &= \mathbb{E}\ \left[\exp\big(iZ^*\Lambda(s,t)Z\big)\right] \\ &= \mathbb{E}\ \left[\exp\big(i(sJ_0+tJ_r)\big)\right] = \det\ \big(I - i\ \Gamma\ \Lambda(s,t)\big)^{-1},\end{aligned} \tag{42}$$

one has the following proposition:

Proposition 5.1.

$$\rho_n^{[2]}(r) = \frac{4}{\pi^2}\int_0^\infty\int_0^\infty \frac{\psi(s,t)}{s^2t^2}dsdt \times \frac{1}{\pi^2\det\Sigma_X}, \tag{43}$$

where

$$\psi(s,t) = 1 - \Re\varphi(s,0) - \Re\varphi(0,t) + \frac{1}{2}\big(\Re\varphi(s,t) + \Re\varphi(s,-t)\big),$$

with φ defined in (42)*.*

The proof is available in Appendix 8.2. The practical calculation of (43) is available in Appendix 8.3. The pair correlation function $g_n^{[2]}$ is the normalization of $\rho_n^{[2]}$ by $\rho_n^{[1]} \times \rho_n^{[1]}$:

$$g_n^{[2]}(r) = \frac{\rho_n^{[2]}(r)}{\rho_n^{[1]}\rho_n^{[1]}}.$$

We remark that the functions $g_1^{[2]}$, $g_2^{[2]}$ and $g_3^{[2]}$ tend to a nonzero constant when r tends to zero as illustrated in Fig. 2 (a), unlike in the holomorphic case $g_0^{[2]}$. Indeed we have the following proposition:

Proposition 5.2. *The pair correlation function $g_n^{[2]}(r)$ converges to a nonzero constant when $r \to 0$, and for $n \geq 0$, one has:*

$$\lim_{r\to 0} g_n^{[2]}(r) = \frac{n(n+1)(n^2+n+1)}{(2n^2+2n+1)^2}.$$

The proof is available in Appendix 8.4. Finally, defining the sequence $(l_n)_{n\geq 0}$ defined for $n \geq 0$:

$$l_n := \frac{n(n+1)(n^2+n+1)}{(2n^2+2n+1)^2},$$

we immediately get that l_n tends to $\frac{1}{4}$. Moreover, the sequence $(l_n)_{n\geq 0}$ is strictly increasing. The proof is available in Appendix 8.5, an illustration of this result, being given in Fig. 2 (b).

5.3. Signed 2-point intensity

In this section, we are interested in computing the signed 2-point intensity:

$$\tilde{\rho}_n^{[2]}(r) := \mathbb{E}[J_0 J_r] p_{f_n(0),f_n(r)}(0,0) = \frac{\mathbb{E}[\omega(Z)]}{\pi^2 \det \Sigma_X}, \tag{44}$$

with

$$\omega(Z) = (|z_1|^2 - |z_2|^2)(|z_3|^2 - |z_4|^2),$$

for which have the following expression:

Proposition 5.3.

$$\tilde{\rho}_n^{[2]}(r) = \frac{(\Gamma_{11} - \Gamma_{22})(\Gamma_{33} - \Gamma_{44}) + |\Gamma_{13}|^2 - |\Gamma_{14}|^2 - |\Gamma_{23}|^2 + |\Gamma_{24}|^2}{\pi^2 \det \Sigma_X}.$$

where Γ *is defined in (38).*

The proof is available in Appendix 8.6.

5.4. Hybrid 2-point intensity

Let us now compute the hybrid 2-point intensity:

$$\hat{\rho}_n^{[2]}(r) := \mathbb{E}[|J_0| J_r] p_{f_n(0),f_n(r)}(0,0) = \frac{\mathbb{E}[|J_0| J_r]}{\pi^2 \det \Sigma_X}.$$

We have showed in (3.2) and (3.3) that the zeros of f_n are invariant by translation and rotation. Then defining the two following transformations :

$$T(z) = z - r, \quad R(z) = e^{i\pi} z,$$

we have:

$$\mathbb{E}[|J_0| J_r] = \mathbb{E}[|J_{T(0)}| J_{T(r)}] = \mathbb{E}[|J_{-r}| J_0] = \mathbb{E}[|J_{R(-r)}| J_{R(0)}] = \mathbb{E}[|J_r| J_0],$$

and one has the following proposition:

Proposition 5.4.

$$\hat{\rho}_n^{[2]}(r) = \frac{2}{\pi} \int_0^\infty \frac{\mathrm{Tr}(\Gamma A_2) - \Re\left(\frac{\mathrm{Tr}(M^{-1}\Gamma A_2)}{\det(M)}\right)}{s^2}\, ds \times \frac{1}{\pi^2 \det \Sigma_X}, \tag{45}$$

where

$$M = I - i\Gamma A_1.$$

The proof is available in Appendix 8.7.

5.5. On the repulsivity of charged zeros

In this section, we will see how different charges behave by computing the 2-point intensity between charges of the same sign as well as the charges of different signs. In what follows, we denote $\rho_n^{[2],++}$, $\rho_n^{[2],--}$ and $\rho_n^{[2],+-}$, the 2-point intensity between zeros charged positively, zeros charged negatively and zeros of different charges respectively.

In order to compute $\rho_n^{[2],++}$, $\rho_n^{[2],--}$ and $\rho_n^{[2],+-}$, we use the different 2-point intensities already computed in the previous sections, indeed one has these relationships:

$$\begin{aligned}
\rho_n^{[2]} &= \mathbb{E}[|J_0 J_r|] = \rho_n^{[2],++} + \rho_n^{[2],--} + 2\rho_n^{[2],+-}, \\
\tilde{\rho}_n^{[2]} &= \mathbb{E}[J_0 J_r] = \rho_n^{[2],++} + \rho_n^{[2],--} - 2\rho_n^{[2],+-}, \\
\hat{\rho}_n^{[2]} &= \mathbb{E}[|J_0|J_r] = \rho_n^{[2],++} - \rho_n^{[2],--},
\end{aligned}$$

therefore the repulsion between different charged zeros

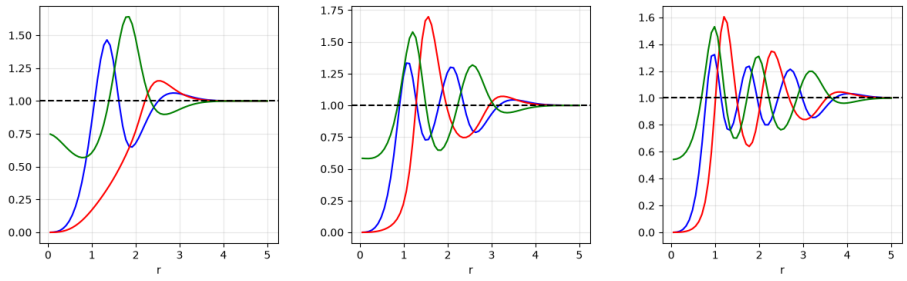
$$\begin{aligned}
\rho_n^{[2],++} &= \frac{1}{2}\left(\frac{\rho_n^{[2]} + \tilde{\rho}_n^{[2]}}{2} + \hat{\rho}_n^{[2]}\right), \\
\rho_n^{[2],--} &= \frac{1}{2}\left(\frac{\rho_n^{[2]} + \tilde{\rho}_n^{[2]}}{2} - \hat{\rho}_n^{[2]}\right), \\
\rho_n^{[2],+-} &= \frac{\rho_n^{[2]} - \tilde{\rho}_n^{[2]}}{4},
\end{aligned}$$

and define the normalized pair correlation function $g_n^{[2],++}$, $g_n^{[2],--}$ and $g_n^{[2],+-}$ as follows:

$$\begin{aligned}
g_n^{[2],++} &= \frac{\rho_n^{[2],++}}{\rho_n^{[1],+}\rho_n^{[1],+}}, \\
g_n^{[2],--} &= \frac{\rho_n^{[2],--}}{\rho_n^{[1],-}\rho_n^{[1],-}}, \\
g_n^{[2],+-} &= \frac{\rho_n^{[2],+-}}{\rho_n^{[1],+}\rho_n^{[1],-}}.
\end{aligned}$$

In Fig. (3), $g_n^{[2],++}$, $g_n^{[2],--}$ and $g_n^{[2],+-}$ are plotted for $n = 1$, $n = 2$ and $n = 3$.

At small scales, the zeros with the same charge represent a strong short-range repulsion. As r increases, this repulsion becomes progressively weaker, as $g_n^{[2],++}$ and $g_n^{[2],--}$ increases to 1. For zeros with opposite charges, the short-range repulsion is weaker as $g_n^{[2],+-}$ remains larger near the origin.



(a) (b) (c)

Figure 3: $g_n^{[2],++}$ (blue), $g_n^{[2],--}$ (red) and $g_n^{[2],+-}$ (green) (a) for $n = 1$ (b) for $n = 2$ and (c) for $n = 3$.

6. Detection of non-degenerate zeros of f_n

In this section, we address the question of how to detect isolated zeros of a function f_n. For $n = 0$, we already know that the zeros of V_{h_0} correspond to the local minima of its spectrogram. For $n \geq 1$, however, not every local minimum corresponds to a zero.

To compute the zeros of f_n, for $n \geq 1$, one may first detect the sign change of both the real and imaginary parts simultaneously within a cell grid. However, this method can miss zeros that are not associated with such a sign change. Also, when the STFT presents high variations, the detection may then fail between consecutive points, which may also affects later the estimation of the Jacobian $\det J_{f_n}$ which depends on the derivatives of $\Re V_{h_n}$ and $\Im V_{h_n}$.

To overcome these limitations, we look at the variation of the complex phase around a point [20, 21]. Indeed, when a contour γ encloses an isolated zero, its image under f_n winds around the origin of the complex plane. This topological property is quantified by the winding number.

6.1. Detection based on winding number

Since a zero is necessarily a local minima, one can first detect all the local minima of the spectrogram and use them as candidate points, and then determine if such a candidate is a zero by studying the phase variation of f_n along a small contour surrounding it. First we define [22]:

Definition 6.1. *If $\gamma : [a, b] \to \mathbb{C}$ is a closed curve, the winding number of γ around $z_0 \in \mathbb{C}$ is defined for $z_0 \notin \gamma([a, b])$ as:*

$$wind(\gamma, z_0) = \frac{1}{2\pi} \Delta_{t\in[a,b]} \arg(\gamma(t) - z_0). \tag{46}$$

So that the winding number measures how many times the curve winds around the point z_0 counted with orientation. In particular, if γ is a positively oriented circle with center at $z_0 \in \mathbb{C}$ and a radius r , ie $\gamma(t) = z_0 + re^{it}$, $t \in$

$[0, 2\pi]$, then [23]:

$$wind(\gamma, z) = \begin{cases} 1, & |z - z_0| < r, \\ 0, & |z - z_0| > r. \end{cases} \tag{47}$$

Now consider f_n and a closed contour γ in the domain of f_n such that $\forall t \in [a, b],\ f_n(\gamma(t)) \neq 0$. Then $f_n \circ \gamma$ is a closed curve in $\mathbb{C}^*$, and the winding number of $f_n \circ \gamma$ around the point 0, corresponds to:

$$wind(f_n \circ \gamma, 0) = \frac{1}{2\pi} \Delta_{t \in [a,b]} \arg(f_n(\gamma(t))),$$

and therefore it measures the total phase variation of f_n along γ.

In practice, the winding number should be approximated by a finite number of samples along the contour. In our approach, these values are not necessarily located on the initial sampling grid. We first construct a separable bicubic interpolation of the real and imaginary part of V_{h_n} [24], and evaluate it on equally separated points on the contour.

Formally, if these points of the contour are denoted by $\zeta_0, \ldots, \zeta_N$, the winding number can be approximated by the discrete sum:

$$wind(V_{h_n} \circ \gamma, 0) \approx \frac{1}{2\pi} \sum_{k=0}^{N-1} \arg\big(\zeta_{k+1} \overline{\zeta_k}\big),\ \zeta_N = \zeta_0.$$

This approximation is based on the assumption that the phase variation between two consecutive samples remains sufficiently small because large phase variations can lead to incorrect estimate of the winding number. To avoid this situation, one can add a criterion on the phase variation proposed by [21], which consists on keeping only points where:

$$\max_{0 \leq k \leq N-1} |\arg\ \big[\zeta_{k+1} \overline{\zeta_k}\big]| < 0.9\pi. \tag{48}$$

In our approach, the bicubic interpolation allows us to evaluate V_{h_n} at an arbitrarily fine number of points along the contour and the angular sampling can be then adjusted to control the phase variations between two successive points.

The radius is then chosen such that the contour encloses only the candidate zero point while avoiding others candidate zeros. The choice of the radius is discussed in the next section.

Algorithm 1 Detection of non-degenerate zeros of f_n

Input: STFT $V_{h_n}\xi$ and a radius R
Compute the local minima of $|V_{h_n}|$
Interpolate $\Re V_{h_n}$ and $\Im V_{h_n}$ using bicubic splines to obtain $\tilde{V}_{h_n}$
for each local minimum z_0 **do**
    Define $\gamma_R(\theta) = z_0 + e^{i\theta}$
    Set $\theta_k = \frac{2\pi k}{N}$ and $\zeta_k = \tilde{V}_{h_n}(\gamma(\theta_k))$
    Compute $wind(V_{h_n} \circ \gamma_R, 0) = \frac{1}{2\pi}\sum_{k=0}^{N-1} \arg\big(\zeta_{k+1}\overline{\zeta_k}\big)$, $\zeta_N = \zeta_0$
    if $|wind(V_{h_n} \circ \gamma_R, 0)| = 1$ **then**
        Accept z_0 as zero and assign charge $\operatorname{sign}(wind(V_{h_n} \circ \gamma_R, 0))$.
    end if
end for

Note that the winding number in our case can only take three values: 1, -1 or 0. To show that, let z_0 be an isolated zero of the polyanalytic function $f(z, \bar{z})$, then near z_0, we may write

$$f(z, \bar{z}) \approx f(z_0, \bar{z}_0) + a(z - z_0) + b(\bar{z} - \bar{z}_0),$$

where $a = \frac{\partial f}{\partial z}(z_0, \bar{z}_0)$ and $b = \frac{\partial f}{\partial \bar{z}}(z_0, \bar{z}_0)$. z_0 is a zero so $f(z_0, \bar{z}_0) = 0$ and on a small circle around z_0, $z = z_0 + re^{i\theta}$ we get:

$$f(z, \bar{z}) \approx are^{i\theta} + bre^{-i\theta} = r(ae^{i\theta} + be^{-i\theta})$$

Writing $a = |a|e^{i\alpha}$ and $b = |b|e^{i\beta}$, one has:

$$f(z, \bar{z}) \approx re^{i\frac{\alpha+\beta}{2}}\left((|a| + |b|)\cos\psi + i(|a| - |b|)\sin\psi\right)$$

where $\psi = \theta + \frac{\alpha-\beta}{2}$.

This shows that the image of a circle is approximately a closed ellipse curve rotated by an angle of $\frac{\alpha+\beta}{2}$ in the complex plane. As θ runs from 0 to 2π, so does ψ, and therefore $\cos\psi$ and $\sin\psi$ each complete one full period. Thus, in the nondegenerate case when $|a| \neq |b|$, and when the contour encloses the simple zero z_0, the point traces the ellipse exactly once and returns to its starting point and the winding number is necessarily $(+1)$ or (-1), according to the sign of

$$J_f(z_0) = |a|^2 - |b|^2.$$

If the contour does not enclose any zero, then the winding number is (0).

6.2. The optimal radius of the contour of the winding numbers for zeros detection

Zeros detection using the proposed algorithm depends strongly on the chosen radius of the contour, indeed a small circle around the zero will detect the corresponding zero, however, as the radius of the circle increases, multiple zeros

will fall into the same contour and the algorithm may fail. To determine the optimal radius of the corresponding contour, we will use densities as a criterion.

Let $\overline{\rho_n^{[1],+}}$ and $\overline{\rho_n^{[1],-}}$ be the estimated average of the positive and negative first-point intensities respectively over a number of realizations and define the following error:

$$E_n(R) = \frac{1}{2}\ (\varepsilon_{n,+} + \varepsilon_{n,-}), \tag{49}$$

where

$$\varepsilon_{n,+} = \frac{\left|\ \overline{\rho_n^{[1],+}} - \rho_n^{[1],+}\right|}{\rho_n^{[1],+}},\ \varepsilon_{n,-} = \frac{\left|\ \overline{\rho_n^{[1],-}} - \rho_n^{[1],-}\right|}{\rho_n^{[1],-}}. \tag{50}$$

The optimal radius is then obtained as:

$$R_n^* = \underset{R>0}{\arg\min}\ E_n(R).$$

We plot the error as a function of the radius R in Fig 4.

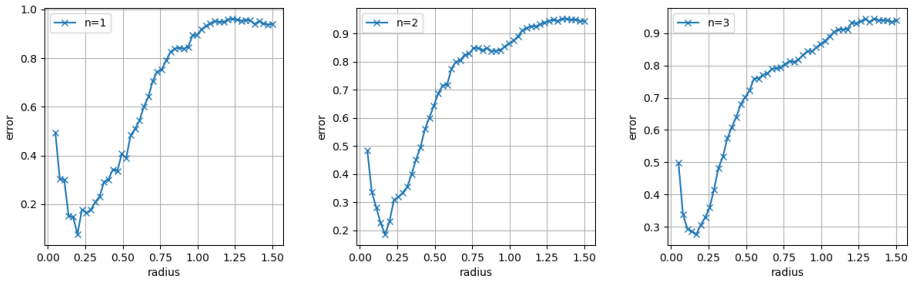
For small values of the radius, the contour is very close to the zero candidate, and the evaluation of the winding number becomes more sensitive to numerical interpolation. As R increases, the estimation becomes more stable leading to a decrease in the error until it reaches a minimum around R_n^*.

However, when $R > R_n^*$, the circle may enclose additional zeros. Since the winding number is additive with respect to the topological charges, its value is then no necessarily equal to ± 1. For example, two zeros with the same charge give a winding number of modulus 2, whereas a zero with charge $+1$ together with a zero with charge -1 gives a winding number of 0.

Thus, the detection criterion $|wind(V_{h_n} \circ \gamma_R, 0)| = 1$, which is designed to a contour containing only one simple zero, may no longer be satisfied when multiple zeros are enclosed, leading to an increase in the detection error for large values of R.

7. Conclusion

In this work, we studied the zeros of the spectrogram of complex white noise analyzed with Hermite windows of order $n \geq 1$, and showed that these zero patterns are statistically organized into two distinct populations, carrying either a positive or a negative charge. We derived closed-form expressions for the one-point intensity and its decomposition by charge, as well as for the unsigned, signed, and hybrid two-point intensities. In particular, we showed that the pair correlation function $r \mapsto g_n^{[2]}(r)$ converges as $r \to 0$ to a strictly positive constant l_n, in contrast with the total repulsion phenomenon observed for the Gaussian window. Finally, we proposed a practical method for detecting the zeros of a spectrogram based on the winding number computed on small circular contours



(a) (b) (c)

Figure 4: The error E_n as a function of the radius r (a): for $n = 1$ (b): for $n = 2$ (c): for $n = 3$

around candidate local minima. As a perspective, we plan to exploit the structure of these zeros to discriminate signal and noise using Delaunay triangulation of zeros according to whether they are charged positively or negatively.

8. Appendix

8.1. Proof of Proposition 2.2

Let us first remark that

$$V_{h_n} h_k(u,-v) = \langle h_k, M_{-v} T_u h_n \rangle = \langle M_v T_u h_n, h_k \rangle = \langle \mathcal{B} M_v T_u h_n, \mathcal{B} h_k \rangle_{\mathcal{F}}. \quad (51)$$

Putting $z_0 = u + iv$, let us first remark that

$$(\mathcal{B} M_v T_u h_n)(z) := e^{-\frac{\pi}{2}|z_0|^2 + i\pi vu} \frac{\pi^{\frac{n}{2}}}{\sqrt{n!}} F(z),$$

where

$$F(z) = e^{\pi z \bar{z_0}} (z - \bar{z_0})^n. \quad (52)$$

To compute (51), using the fact that $\mathcal{B} h_k(z) = \sqrt{\frac{\pi^k}{k!}} z^k$ is an orthonormal basis in $\mathcal{F}$, we identify the coefficient of z^k in $F(z)$, denoted by $[z^k]F(z)$, and then multiply it by $\sqrt{\frac{k!}{\pi^k}}$. Writing the binomial expansion of $(z - \bar{z}_0)^n$ and the Taylor series of $e^{\pi z \bar{z_0}}$:

$$(z - \bar{z}_0)^n = \sum_{i=0}^{n} \binom{n}{i} (-\bar{z}_0)^{n-i} z^i, \; e^{\pi z \bar{z_0}} = \sum_{p=0}^{\infty} \frac{(\pi z_0)^p}{p!} z^p.$$

Hence

$$F(z) = \sum_{i=0}^{n} \binom{n}{i} (-\bar{z}_0)^{n-i} \sum_{p=0}^{\infty} \frac{(\pi z_0)^p}{p!} z^{i+p}.$$

The coefficient of z^k is obtained by setting $p = k - i$, which requires $0 \leq i \leq \min(n, k)$:

$$[z^k]\, F(z) = \sum_{i=0}^{\min(n,k)} \binom{n}{i} \frac{(-\bar{z}_0)^{n-i} (\pi z_0)^{k-i}}{(k-i)!}.$$

Re-indexing $j = k - i$, then the sum goes from $\max(0, k-n)$ to k, one gets:

$$[z^k]\, F(z) = \sum_{j=\max(0,k-n)}^{k} \binom{n}{k-j} \frac{(-\bar{z}_0)^{n-k+j} (\pi z_0)^{j}}{j!}.$$

If $k \leq n$,

$$[z^k]\, F(z) \quad = \quad (-\bar{z}_0)^{n-k} \sum_{j=0}^{k} \binom{n}{k-j} \frac{(-\pi |z_0|^2)^j}{j!},$$

which corresponds to the standard form of the generalized Laguerre polynomial

$$L_n^{(\alpha)}(x) = \sum_{j=0}^{n} \binom{n+\alpha}{n-j} \frac{(-x)^j}{j!}.$$

So for $k < n$,

$$\langle \mathcal{B} M_v T_u h_n, \mathcal{B} h_k \rangle_{\mathcal{F}} = e^{-\frac{\pi}{2}|z_0|^2 + i\pi vu} \sqrt{\frac{\pi^{n-k} k!}{n!}} (-\bar{z}_0)^{n-k} L_k^{(n-k)}(\pi |z_0|^2).$$

Now if $k > n$,

$$[z^k]\, F(z) = \sum_{j=k-n}^{k} \binom{n}{k-j} \frac{(-\bar{z}_0)^{n-k+j} (\pi z_0)^{j}}{j!}.$$

Re-indexing this time $m = j - k + n$, one gets:

$$[z^k]\, F(z) = {z_0}^{k-n} \pi^{k-n} \sum_{m=0}^{n} \binom{n}{m} \frac{(-\pi |z_0|^2)^m m!}{m!(m+k-n)!}.$$

As $\binom{n}{m} \frac{m!}{(m+k-n)!} = \frac{n!}{k!} \binom{k}{n-m}$, one obtains:

$$[z^k]\, F(z) = {z_0}^{k-n} \frac{\pi^k}{\pi^n} \frac{n!}{k!} \sum_{m=0}^{n} \binom{k}{n-m} \frac{(-\pi |z_0|^2)^m}{m!}.$$

Thus

$$\langle \mathcal{B} M_v T_u h_n, \mathcal{B} h_k \rangle_{\mathcal{F}} = e^{-\frac{\pi}{2}|z_0|^2 + i\pi vu} \sqrt{\frac{\pi^{k-n} n!}{k!}} z_0^{k-n} L_n^{(k-n)}(\pi |z_0|^2).$$

8.2. Proof of Proposition 5.1

For every $s, t \in \mathbb{R}$, using we recall that

$$\varphi(s,t) = \mathbb{E}\ \left[\exp\big(i(sJ_0 + tJ_r)\big)\right]. \tag{53}$$

Using the Dirichlet integral

$$\int_0^\infty \frac{\sin(x)}{x}\ dx = \frac{\pi}{2},$$

one can prove that for all $x \in \mathbb{R}$:

$$|x| = \frac{2}{\pi}\int_0^\infty \frac{1-\cos(sx)}{s^2}\ ds.$$

Applying this to both J_0 and J_r, we obtain:

$$|J_0| = \frac{2}{\pi}\int_0^\infty \frac{1-\cos(sJ_0)}{s^2}\ ds,\ |J_r| = \frac{2}{\pi}\int_0^\infty \frac{1-\cos(sJ_r)}{s^2}\ ds, \tag{54}$$

therefore

$$\begin{aligned} |J_0 J_r| &= \frac{4}{\pi^2}\iint_{(\mathbb{R}^+)^2} \frac{\big(1-\cos(sJ_0)\big)\big(1-\cos(tJ_r)\big)}{s^2t^2}\ ds\ dt \\ &= \frac{4}{\pi^2}\iint_{(\mathbb{R}^+)^2} \frac{1-\cos(sJ_0)-\cos(tJ_r)+\cos(sJ_0)\cos(tJ_r)}{s^2t^2}\ ds\ dt. \end{aligned}$$

Then using

$$\cos(sJ_0)\cos(tJ_r) = \frac{1}{2}\big(\cos(sJ_0+tJ_r)+\cos(sJ_0-tJ_r)\big),$$

and

$$\mathbb{E}\ \left[\cos\big(sJ_0+tJ_r\big)\right] = \Re\varphi(s,t),$$

one obtains

$$\mathbb{E}\ \left[|J_0J_r|\right] = \frac{4}{\pi^2}\int_0^\infty\int_0^\infty \frac{\psi(s,t)}{s^2t^2}dsdt,$$

where

$$\psi(s,t) = 1 - \Re\varphi(s,0) - \Re\varphi(0,t) + \frac{1}{2}\big(\Re\varphi(s,t)+\Re\varphi(s,-t)\big),$$

which ends the proof.

8.3. Implementation details

The integral

$$J := \int_0^\infty \int_0^\infty \frac{\psi(s,t)}{s^2 t^2} ds dt, \tag{55}$$

is theoretically correct, but in practice becomes rapidly numerically unstable when r increases. In order to explain this, let us consider the integral

$$\frac{\pi}{2}|x| = I(x) = \int_0^\infty \frac{1-\cos(sx)}{s^2} ds.$$

When $|x|$ is too large, $s \to \cos(sx)$ varies rapidly, indeed, its zeros and the distance between two consecutive zeros are given respectively by:

$$s_k = \frac{(2k+1)\pi}{2|x|} \text{ and } s_{k+1} - s_k = \frac{\pi}{|x|}.$$

Thus the variations of $\cos(sx)$ are located in intervals of length proportional to $\frac{1}{|x|}$ and a numerical discretization must see such variations which becomes numerically difficult especially in our case when $|x|$ is large.

To overcome this problem, we make the change of variable $u = |x|s$ and the integral becomes

$$I(x) = |x| \int_0^\infty \frac{1-\cos(u)}{u^2} du,$$

and the variations inside the integral no longer depend on x. In our case, the changes of variable that should be done are $u = |J_0|s = \sqrt{J_0^2}s$ and $v = |J_r|t = \sqrt{J_r^2}t$, but since J_0 and J_r are random realizations, we consider instead

$$u = \sqrt{\mathbb{E}[J_0^2]}s, \; v = \sqrt{\mathbb{E}[J_r^2]}t,$$

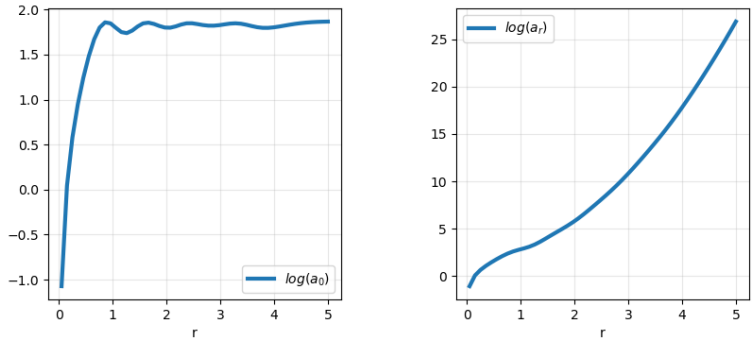
and the integral (55) becomes

$$J = a_0 a_r \int_0^\infty \int_0^\infty \frac{\psi(\frac{u}{a_0}, \frac{v}{a_r})}{u^2 v^2} du dv.$$

To compute the quantities a_0 and a_r, we use the following result:

Proposition 8.1. *Let us consider a Gaussian vector Z with covariance matrix Γ and a Hermitian matrix A, one has:*

$$\mathbb{E}[(Z^* A Z)^2] \quad = \quad (\mathrm{Tr}(\Gamma A))^2 + \mathrm{Tr}(\Gamma A \Gamma A) \tag{56}$$



(a) (b)

Figure 5: Logarithmic plots of (a) a_0 and (b) a_r as function of r.

Proof. We have

$$(Z^*AZ)^2 = \left(\sum_{i,j} \bar{z}_i A_{i,j} z_j\right)^2 = \sum_{i,j}\sum_{k,l} \bar{z}_i A_{i,j} z_j \bar{z_k} A_{k,l} z_l,$$

then introducing the expectation

$$\mathbb{E}[(Z^*AZ)^2] = \sum_{i,j}\sum_{k,l} A_{i,j} A_{k,l} \mathbb{E}[\bar{z}_i z_j \bar{z_k} z_l],$$

and using Isserlis's theorem [25]

$$\mathbb{E}[\bar{z}_i z_j \bar{z_k} z_l] = \Gamma_{i,j}\Gamma_{k,l} + \Gamma_{i,l}\Gamma_{k,j},$$

we obtain

$$\begin{aligned}
\mathbb{E}[(Z^*AZ)^2] &= \sum_{i,j}\sum_{k,l} A_{i,j} A_{k,l} \Gamma_{i,j}\Gamma_{k,l} + \sum_{i,j}\sum_{k,l} A_{i,j} A_{k,l} \Gamma_{i,l}\Gamma_{k,j} \\
&= \sum_{i,j} A_{i,j}\Gamma_{i,j} \sum_{k,l} A_{k,l}\Gamma_{k,l} + \sum_{i,j}\sum_{k,l} A_{i,j} A_{k,l} \Gamma_{i,l}\Gamma_{k,j} \\
&= \left(\sum_{i,j} A_{i,j}\Gamma_{i,j}\right)^2 + \sum_{i,j}\sum_{k,l} A_{i,j} A_{k,l} \Gamma_{i,l}\Gamma_{k,j}.
\end{aligned}$$

On the other hand, and using the symmetry of Γ

$$\mathrm{Tr}(A\Gamma) = \sum_i (A\Gamma)_{i,i} = \sum_{i,j} A_{i,j}\Gamma_{j,i} = \sum_{i,j} A_{i,j}\Gamma_{i,j},$$

and

$$\begin{aligned}\mathrm{Tr}(A\Gamma A\Gamma) &= \sum_{i,k}(A\Gamma)_{i,k}(A\Gamma)_{k,i} = \sum_{i,k}\sum_{j} A_{i,j}\Gamma_{j,k}\sum_{l} A_{k,l}\Gamma_{l,i} \\ &= \sum_{i,j,k,l} A_{i,j}\Gamma_{j,k}A_{k,l}\Gamma_{l,i} = \sum_{i,j,k,l} A_{i,j}A_{k,l}\Gamma_{j,k}\Gamma_{l,i}.\end{aligned}$$

Therefore

$$\mathbb{E}[(Z^*AZ)^2] = \left(\mathrm{Tr}(A\Gamma)\right)^2 + \mathrm{Tr}(A\Gamma A\Gamma) = \left(\mathrm{Tr}(\Gamma A)\right)^2 + \mathrm{Tr}(\Gamma A\Gamma A).$$

□

The two quantities a_0 and a_r are then given by:

$$\begin{aligned}a_0^2 = \mathbb{E}[J_0^2] &= \left(\mathrm{Tr}(\Gamma A_1)\right)^2 + \mathrm{Tr}(\Gamma A_1\Gamma A_1), \\ a_r^2 = \mathbb{E}[J_r^2] &= \left(\mathrm{Tr}(\Gamma A_2)\right)^2 + \mathrm{Tr}(\Gamma A_2\Gamma A_2).\end{aligned}$$

In Fig. 5, the logarithms of a_0 and a_r are plotted, motivating the changes of variable explained above.

8.4. Proof of the monotonicity of l_n

Define the sequence $(x_n)_{n\geq 0}$ and the function ϕ respectively by

$$x_n = \frac{n(n+1)}{(2n+1)^2} \text{ and } \phi(n) = n(n+1).$$

One then remarks that $\phi(n)$ is strictly increasing and that:

$$l_n = \frac{n(n+1)(n^2+n+1)}{(2n^2+2n+1)^2} = x_{\phi(n)}.$$

So to prove that l_n is increasing it is sufficient to prove that x_n is increasing, thus we compute

$$\begin{aligned}x_{n+1} - x_n &= \tfrac{(n+1)(n+2)}{(2n+3)^2} - \tfrac{n(n+1)}{(2n+1)^2} = (n+1)\left(\tfrac{n+2}{(2n+3)^2} - \tfrac{n}{(2n+1)^2}\right) \\ &= (n+1)\left(\tfrac{(n+2)(2n+1)^2 - n(2n+3)^2}{(2n+3)^2(2n+1)^2}\right) = \tfrac{2(n+1)}{(2n+3)^2(2n+1)^2} > 0,\end{aligned}$$

which ends the proof.

8.5. Proof of Proposition 5.2

In order to compute

$$\lim_{r\to 0} g_n^{[2]}(r),$$

we need to compute the asymptotics, when r is small, of:

$$\det \Sigma_X(r) \text{ and } \mathbb{E}[|J_0 J_r|].$$

Let us consider $n \geq 0$ and put $x = r^2$. We have the following Taylor expansions:

$$L^{[0]} = L_n(x) = 1 - nx + \frac{n(n-1)}{4}x^2 + O(x^4),\ e^x = 1 + x + \frac{x^2}{2} + O(x^3),$$

and thus

$$\Delta = \det \Sigma_X(r) = e^x - (L^{[0]})^2 = (2n+1)x + \frac{1+n-3n^2}{2}x^2 + O(x^3). \quad (57)$$

Then, to compute $\mathbb{E}[|J_0 J_r|]$ when r is small we first compute first order in x of Γ. For that purpose we first compute

$$L^{[1]} = L_n'(x) = -n + \frac{n(n-1)}{2}x + O(x^2),\ L^{[2]} = L_n''(x) = \frac{n(n-1)}{2} + O(x),$$
$$B^{[0]} = L^{[0]} - L^{[1]} = n + 1 - \frac{n(n+1)}{2}x + O(x^2),$$
$$B^{[1]} = L^{[1]} - L^{[2]} = -\frac{n(n+1)}{2} + O(x).$$

Recalling that

$$\Gamma \quad = \sum_Y - (\sum_0)^H (\sum_X)^{-1} \sum_0,$$

we denote the columns of Σ_0 defined in (59) by c_1, c_2, c_3, c_4, namely

$$c_1 = \begin{pmatrix} 0 \\ rB^{[0]} \end{pmatrix},\ c_2 = \begin{pmatrix} 0 \\ -rL^{[1]} \end{pmatrix},\ c_3 = \begin{pmatrix} rL^{[1]} \\ re^{r^2} \end{pmatrix}, c_4 = \begin{pmatrix} rL^{[1]} \\ 0 \end{pmatrix},$$

and Σ_X^{-1} reads:

$$\Sigma_X^{-1} = \frac{1}{\Delta} \begin{pmatrix} e^x & -L^{[0]} \\ -L^{[0]} & 1 \end{pmatrix}.$$

Considering the definition (60) of Σ_Y, we compute the expansion of Γ_{11}:

$$\Gamma_{11} = (\Sigma_Y)_{11} - c_1^T \Sigma_X^{-1} c_1 = n + 1 - \frac{x(B^{[0]})^2}{\Delta}.$$

Using the expression of Δ introduced above and since

$$x(B^{[0]})^2 = (n+1)^2 x - n(n+1)^2 x^2 + O(x^3),$$

we get, after some simple computations, that

$$c_1^T \Gamma_X^{-1} c_1 \quad = \tfrac{(n+1)^2}{(2n+1)} - \tfrac{(n+1)^2(n^2+3n+1)}{2(2n+1)^2}x + O(x^2).$$

Therefore:

$$\Gamma_{11} = \frac{n(n+1)}{(2n+1)} + \frac{(n+1)^2(n^2+3n+1)}{2(2n+1)^2} r^2 + O(r^4).$$

Similarly, we may write:

$$\begin{aligned}
\Gamma_{12} &= (\Sigma_Y)_{12} - c_1^T \Sigma_X^{-1} c_2 = \frac{xB^{[0]}L^{[1]}}{\Delta} = -\frac{n(n+1)}{(2n+1)} + \frac{n^2(n+1)^2}{2(2n+1)^2} r^2 + O(r^4) \\
\Gamma_{22} &= (\Sigma_Y)_{22} - c_2^T \Sigma_X^{-1} c_2 = n - \frac{x(L^{[1]})^2}{\Delta} = \frac{n(n+1)}{(2n+1)} + \frac{n^2(n^2-n-1)}{2(2n+1)^2} r^2 + O(r^4) \\
\Gamma_{13} &= (\Sigma_Y)_{13} - c_1^T \Sigma_X^{-1} c_3 = n+1-n(n+1)x + O(x^2) - \frac{xB^{[0]}(e^x - L^{[1]}L^{[0]})}{\Delta} \\
&= \frac{n(n+1)}{(2n+1)} - \frac{(n+1)^2(3n^2+3n+1)}{2(2n+1)^2} r^2 + O(r^4) \\
\Gamma_{23} &= (\Sigma_Y)_{23} - c_2^T \Sigma_X^{-1} c_3 = -\frac{n(n+1)}{2} x + O(x^2) + \frac{xL^{[1]}(e^x - L^{[0]}L^{[1]})}{\Delta} \\
&= -\frac{n(n+1)}{(2n+1)} + \frac{n(n+1)(n^2-n-1)}{2(2n+1)^2} r^2 + O(r^4) \\
\Gamma_{33} &= (\Sigma_Y)_{33} - c_3^T \Sigma_X^{-1} c_3 \\
&= n+1+(n+2)x + O(x^2) - \frac{x(e^x(L^{[1]})^2 - 2L^{[0]}L^{[1]}e^x + e^{2x})}{\Delta} \\
\Gamma_{14} &= (\Sigma_Y)_{14} - c_1^T \Sigma_X^{-1} c_4 = -\frac{n(n+1)}{2} x + O(x^2) + \frac{xB^{[0]}L^{[1]}L^{[0]}}{\Delta} \\
&= -\frac{n(n+1)}{(2n+1)} + \frac{n(n+1)(n^2-n-1)}{2(2n+1)^2} r^2 + O(r^4) \\
\Gamma_{24} &= (\Sigma_Y)_{24} - c_2^T \Sigma_X^{-1} c_4 = n - n(n-1)x + O(x^2) + \frac{x(L^{[1]})^2 L^{[0]}}{\Delta} \\
&= \frac{n(n+1)}{(2n+1)} - \frac{n(3n+2)(n^2-n-1)}{2(2n+1)^2} r^2 + O(r^4) \\
\Gamma_{34} &= (\Sigma_Y)_{34} - c_3^T \Sigma_X^{-1} c_4 = -\frac{xe^x L^{[1]}(L^{[1]} - L^{[0]})}{\Delta} \\
&= -\frac{n(n+1)}{(2n+1)} + \frac{n(n+1)(n^2-3n-2)}{2(2n+1)^2} r^2 + O(r^4) \\
\Gamma_{44} &= (\Sigma_Y)_{44} - c_4^T \Sigma_X^{-1} c_4 = n + nx + O(x^2) - \frac{xe^x(L^{[1]})^2}{\Delta} \\
&= \frac{n(n+1)}{(2n+1)} + \frac{n(n^3+3n^2+5n+2)}{2(2n+1)^2} r^2 + O(r^4)
\end{aligned}$$

Now let introduce the quantities

$$D_0 = z_1 - z_2,\ S_0 = z_1 + z_2,\ D_1 = z_3 - z_4,\ S_1 = z_3 + z_4.$$

One first remark that

$$J_0 = \Re(\overline{D_0}S_0),\ J_r = \Re(\overline{D_1}S_1)$$

and thus $\mathbb{E}[|J_0 J_r|] = \mathbb{E}[|\Re(\overline{D_0}S_0)\Re(\overline{D_1}S_1)|]$. Let us first study D_0 and D_1, for which we have:

$$\mathbb{E}[|D_0|^2] = \Gamma_{11} + \Gamma_{22} - 2\Gamma_{12} = \frac{4n(n+1)}{2n+1} + O(r^2),$$
$$\mathbb{E}[|D_1|^2] = \Gamma_{33} + \Gamma_{44} - 2\Gamma_{34} = \frac{4n(n+1)}{2n+1} + O(r^2),$$
$$\mathbb{E}[D_0\overline{D_1}] = \Gamma_{13} + \Gamma_{24} - \Gamma_{14} - \Gamma_{23} = \frac{4n(n+1)}{2n+1} + O(r^2).$$

From this we deduce that

$$\mathbb{E}[|D_1 - D_0|^2] \underset{r\to 0}{\longrightarrow} 0.$$

Furthermore as Z is a Gaussian vector that converges in distribution to $\mathcal{CN}(0, \Gamma_0)$, where Γ_0 is the limit of Γ when r tends to 0. D_0 converges in distribution to $\mathcal{CN}(0, A^T\Gamma_0 A)$, with $A = (1, -1, 0, 0)^T$. Similarly D_1 converges in distribution to $\mathcal{CN}(0, B^T\Gamma_0 B)$, with $B = (0, 0, 1, -1)^T$. Now, we can prove that D_0 and D_1 converge to the same distribution. Indeed, let us recall for consistency:

Theorem 8.1 (Slutsky's theorem, [26] p.239)**.** *Let X_n and Y_n be sequences of random elements. If X_n converges in distribution to a random variable X and Y_n converges in probability to a constant c, then:*

$$X_n + Y_n \xrightarrow{d} X + c.$$

In our case, assume $D_0 \xrightarrow{d} D$ and $D_1 \xrightarrow{d} \tilde{D}$ then we also have

$$D_1 = D_0 + D_1 - D_0 \xrightarrow{d} D,$$

since $D_0 \xrightarrow{d} D$, $D_1 - D_0 \xrightarrow{L^2} 0$ and thus also in probability, and finally applying Slutsky's theorem. Let us call D the common limit of D_0 and D_1.

Now let us consider the variables S_0 and S_1, for which we have:

$$\mathbb{E}[|S_0|^2] = \Gamma_{11} + \Gamma_{22} + 2\Gamma_{12} = \frac{n^2+n+1}{2}r^2 + O(r^4),$$
$$\mathbb{E}[|S_1|^2] = \Gamma_{33} + \Gamma_{44} + 2\Gamma_{34} = \frac{n^2+n+1}{2}r^2 + O(r^4),$$
$$\mathbb{E}[S_0\overline{S_1}] = \Gamma_{13} + \Gamma_{14} + \Gamma_{23} + \Gamma_{24} = -\frac{n^2+n+1}{2}r^2 + O(r^4).$$

Now let us define the variables $\tilde{S_0} = \frac{S_0}{r}$ and $\tilde{S_1} = \frac{S_1}{r}$, which are Gaussian variable converging in distribution to $\tilde{S}$ and $\tilde{\tilde{S}}$ respectively. From the equalities

just above we have

$$\mathbb{E}[|\tilde{S_0}+\tilde{S_1}|^2]=\mathbb{E}[|\tilde{S_0}|^2]+\mathbb{E}[|\tilde{S_1}|^2]+2\Re\mathbb{E}[\tilde{S_0}\overline{\tilde{S_1}}]\underset{r\to 0}{\longrightarrow}0.$$

Using the same reasoning before, we write:

$$\tilde{S_1}=-\tilde{S_0}+\tilde{S_1}+\tilde{S_0}\xrightarrow{d}-\tilde{S}.$$

Now let us compute

$$\mathbb{E}[D_0\overline{S_0}]=\Gamma_{11}-\Gamma_{22}=O(r^2),\ \mathbb{E}[D_r\overline{S_r}]=\Gamma_{33}-\Gamma_{44}=O(r^2),$$

which means that the variables D_0 and $\tilde{S_0}$ are asymptotically independent. Similarly, D_1 and $\tilde{S_1}$ are asymptotically independent. Therefore we can write

$$\frac{J_0}{r}\xrightarrow{d}\Re(\overline{D}\tilde{S}),\ \frac{J_r}{r}\xrightarrow{d}-\Re(\overline{D}\tilde{S}),$$

therefore

$$\frac{|J_0J_r|}{r^2}\xrightarrow{d}\left[\Re(\overline{D}\tilde{S})\right]^2.$$

Putting $D=D_x+iD_y$ and $\tilde{S}=\tilde{S}_x+i\tilde{S}_y$ then

$$\left[\Re(\overline{D}\tilde{S})\right]^2=D_x^2\tilde{S}_x^2+D_y^2\tilde{S}_y^2-2D_xD_y\tilde{S}_x\tilde{S}_y.$$

Since the variables D and $\tilde{S}$ are circular symmetric Gaussian variables, then:

$$\mathbb{E}[D_xD_y]=\mathbb{E}[\tilde{S}_x\tilde{S}_y]=0,$$

and

$$\mathbb{E}[D_x^2]=\mathbb{E}[D_y^2]=\frac{1}{2}\mathbb{E}[|D|^2],\ \mathbb{E}[\tilde{S}_x^2]=\mathbb{E}[\tilde{S}_y^2]=\frac{1}{2}\mathbb{E}[|\tilde{S}|^2].$$

Using Isserlis's theorem, and asymptotic independence, we get

$$\begin{aligned}\mathbb{E}[D_x^2\tilde{S}_x^2] &= \mathbb{E}[D_x^2]\mathbb{E}[\tilde{S}_x^2],\\ \mathbb{E}[D_y^2\tilde{S}_y^2] &= \mathbb{E}[D_y^2]\mathbb{E}[\tilde{S}_y^2],\\ \mathbb{E}[D_xD_y\tilde{S}_x\tilde{S}_y] &= 0.\end{aligned}$$

Combining all these results, one obtains :

$$\frac{\mathbb{E}[|J_0J_r|]}{r^2}\underset{r\to 0}{\longrightarrow}\frac{1}{2}\mathbb{E}[|D|^2]\mathbb{E}[|S|^2]=\frac{n(n+1)(n^2+n+1)}{(2n+1)},$$

and using (57),

$$\frac{\det \Sigma_X}{r^2} \underset{r\to 0}{\longrightarrow} (2n+1),$$

one gets that

$$\rho_n^{[2]}(r) = \frac{\mathbb{E}[|J_0 J_r|]}{\pi^2 \det \Sigma_X} \underset{r\to 0}{\longrightarrow} \frac{n(n+1)(n^2+n+1)}{(2n+1)^2\pi^2}.$$

Also we know that (35):

$$\rho_n^{[1]} = \frac{1}{\pi}(n+1/2+\frac{1}{4n+2}) = \frac{1}{\pi}\ \frac{4n^2+4n+2}{2(2n+1)} = \frac{1}{\pi}\ \frac{2n^2+2n+1}{2n+1}.$$

Thus

$$g_n^{[2]}(r) = \frac{\rho_n^{[2]}(r)}{\rho_n^{[1]}\rho_n^{[1]}} \underset{r\to 0}{\longrightarrow} \frac{n(n+1)(n^2+n+1)}{(2n^2+2n+1)^2},$$

which concludes the proof.

8.6. Proof of Proposition 5.3

Let us first start computing the covariance matrix of Z. The kernel we consider here is $\tilde{K}^n(z,w) = L_n(|z-w|^2)e^{z\bar{w}}$. Putting $L_n^{(i)} = L_n^{(i)}(r^2)$, $i \geq 0$, we get:

$$\Sigma_X = \begin{pmatrix} \tilde{K}^n(0,0) & \tilde{K}^n(0,r) \\ \tilde{K}^n(r,0) & \tilde{K}^n(r,r) \end{pmatrix} = \begin{pmatrix} 1 & L_n \\ L_n & e^{r^2} \end{pmatrix},$$

and thus

$$\Sigma_X^{-1} = \frac{1}{e^{r^2}-L_n^2}\begin{pmatrix} e^{r^2} & -L_n \\ -L_n & 1 \end{pmatrix}. \tag{58}$$

We then have

$$\partial_w \tilde{K}^n(z,w) \quad = \quad \mathbb{E}[f_n(z)\overline{\partial_{\bar{w}} f_n(w)}].$$

Therefore

$$\begin{aligned} \sum\nolimits_0 = \begin{pmatrix} \partial_{\bar{w}}\tilde{K}^n(0,0) & \partial_w\tilde{K}^n(0,0) & \partial_{\bar{w}}\tilde{K}^n(0,r) & \partial_w\tilde{K}^n(0,r) \\ \partial_{\bar{w}}\tilde{K}^n(r,0) & \partial_w\tilde{K}^n(r,0) & \partial_{\bar{w}}\tilde{K}^n(r,r) & \partial_w\tilde{K}^n(r,r) \end{pmatrix} \\ = \begin{pmatrix} 0 & 0 & rL_n' & rL_n' \\ rB^{[0]} & -rL_n' & re^{r^2} & 0 \end{pmatrix}, \end{aligned} \tag{59}$$

in which $B^{[0]} = L_n(r^2) - L_n'(r^2)$. Finally for $\Sigma_Y = \mathbb{E}[YY^H]$, we first write that:

$$\partial^2_{z,w}\tilde{K}^n(z,w) \quad = \quad \mathbb{E}[\partial_z f_n(z)\partial_w\overline{f_n(w)}],$$

and then, putting $B^{[i]} = L_n^{(i)} - L_n^{(i+1)}$ and remarking that $L_n(0) = 1$, $L_n'(0) = -n$, we get:

$$\Sigma_Y = \begin{pmatrix} \partial^2_{z,\bar{w}}\tilde{K}^n(0,0) & \partial^2_{z,w}\tilde{K}^n(0,0) & \partial^2_{z,\bar{w}}K^n(0,r) & \partial^2_{z,w}\tilde{K}^n(0,r) \\ \partial^2_{\bar{z},\bar{w}}\tilde{K}^n(0,0) & \partial^2_{\bar{z},w}\tilde{K}^n(0,0) & \partial^2_{\bar{z},\bar{w}}\tilde{K}^n(0,r) & \partial^2_{\bar{z},w}\tilde{K}^n(0,r) \\ \partial^2_{z,\bar{w}}\tilde{K}^n(r,0) & \partial^2_{z,w}\tilde{K}^n(r,0) & \partial^2_{z,\bar{w}}\tilde{K}^n(r,r) & \partial^2_{z,w}\tilde{K}^n(r,r) \\ \partial^2_{\bar{z},\bar{w}}\tilde{K}^n(r,0) & \partial^2_{\bar{z},w}\tilde{K}^n(r,0) & \partial^2_{\bar{z},\bar{w}}\tilde{K}^n(r,r) & \partial^2_{\bar{z},w}\tilde{K}^n(r,r) \end{pmatrix} = \begin{pmatrix} n+1 & 0 & r^2B^{[1]} + B^{[0]} & r^2B^{[1]} \\ 0 & n & -r^2L_n'' & -r^2L_n'' - L_n' \\ r^2B^{[1]} + B^{[0]} & -r^2L_n'' & (n+1+r^2)e^{r^2} & 0 \\ r^2B^{[1]} & -r^2L_n'' - L_n' & 0 & ne^{r^2} \end{pmatrix}. \tag{60}$$

Then the variable Z is zero mean Gaussian vector with covariance matrix

$$\Gamma \quad = \sum_Y - (\sum_0)^H (\sum_X)^{-1} \sum_0,$$

and then

$$J_{f_n(z)} = |\partial_z f_n(z)|^2 - |\partial_{\bar{z}} f_n(z)|^2 := \omega(Z),$$

which we rewrite as

$$\omega(Z) = (|z_1|^2 - |z_2|^2)(|z_3|^2 - |z_4|^2),$$

putting $Z = (z_1, \ldots, z_4)$. Then developing $\varphi(Z)$, we get:

$$\mathbb{E}[\omega(Z)] = \mathbb{E}[|z_1|^2|z_3|^2] - \mathbb{E}[|z_1|^2|z_4|^2] - \mathbb{E}[|z_2|^2|z_3|^2] + \mathbb{E}[|z_2|^2|z_4|^2].$$

As Z is a Gaussian vector we have $z_i \sim e^{i\theta} z_i$, and thus

$$\mathbb{E}[z_i^2] = \mathbb{E}[e^{2i\theta} z_i^2] = e^{2i\theta}\mathbb{E}[z_i^2] = 0, \ \mathbb{E}[z_i z_j] = \mathbb{E}[e^{2i\theta} z_i z_j] = e^{2i\theta}\mathbb{E}[z_i z_j] = 0.$$

Then using the Isserlis' theorem [25]:

$$\begin{aligned} \mathbb{E}[|z_i|^2|z_j|^2] &= \mathbb{E}[z_i\bar{z}_i z_j\bar{z}_j] = \mathbb{E}[z_i\bar{z}_i]\mathbb{E}[z_j\bar{z}_j] + \mathbb{E}[z_i z_j]\mathbb{E}[\bar{z}_i\bar{z}_j] + \mathbb{E}[z_i\bar{z}_j]\mathbb{E}[\bar{z}_i z_j] \\ &= \mathbb{E}[|z_i|^2]\mathbb{E}[|z_j|^2] + |\mathbb{E}[z_i z_j]|^2 + |\mathbb{E}[z_i\bar{z}_j]|^2 = \mathbb{E}[|z_i|^2]\mathbb{E}[|z_j|^2] + |\mathbb{E}[z_i\bar{z}_j]|^2 \end{aligned}$$

Finally, denoting by $\Gamma = \mathrm{Cov}(Z)$, and $\Omega_{ij} = \mathbb{E}[z_i z_j]$, one obtains:

$$\begin{aligned} \mathbb{E}[|z_1|^2|z_3|^2] &= \Gamma_{11}\Gamma_{33} + |\Gamma_{13}|^2, \quad \mathbb{E}[|z_1|^2|z_4|^2] = \Gamma_{11}\Gamma_{44} + |\Gamma_{14}|^2, \\ \mathbb{E}[|z_2|^2|z_3|^2] &= \Gamma_{22}\Gamma_{33} + |\Gamma_{23}|^2, \quad \mathbb{E}[|z_2|^2|z_4|^2] = \Gamma_{22}\Gamma_{44} + |\Gamma_{24}|^2. \end{aligned}$$

Then reinjecting these expressions in the conditional expectation we obtain:

$$\mathbb{E}[\omega(Z)] = (\Gamma_{11} - \Gamma_{22})(\Gamma_{33} - \Gamma_{44}) + |\Gamma_{13}|^2 - |\Gamma_{14}|^2 - |\Gamma_{23}|^2 + |\Gamma_{24}|^2.$$

8.7. Proof of Proposition 5.4

Using (54), and multiplying it by J_r:

$$|J_0|\, J_r = \frac{2}{\pi} \int_0^\infty \frac{J_r - J_r\ \cos(sJ_0)}{s^2}\ ds,$$

then

$$\mathbb{E}[|J_0|\, J_r] = \frac{2}{\pi} \int_0^\infty \frac{\mathbb{E}[J_r] - \mathbb{E}[J_r\ \cos(sJ_0)]}{s^2}\ ds.$$

For $\mathbb{E}[J_r]$, we have:

$$\mathbb{E}[J_r] = \mathbb{E}[Z^* A_2 Z] = \sum_{i,j} (A_2)_{i,j} \Gamma_{i,j} = \mathrm{Tr}(\Gamma A_2),$$

and in order to compute $\mathbb{E}[J_r\ \cos(sJ_0)]$, we use the function $(s,t) \to \varphi(s,t)$ defined in (42), indeed:

$$\partial_t \varphi(s,0) = \mathbb{E}[iJ_r e^{isJ_0}],$$

therefore

$$\mathbb{E}[J_r \cos(sJ_0)] = \Im(\partial_t \varphi(s,0)).$$

Consider $M = I - i\ \Gamma\ (sA_1 + tA_2)$ and using Jacobi's formula:

$$\begin{aligned} \partial_t \varphi(s,t) &= \frac{-\det(M)\ \mathrm{Tr}(M^{-1}\ (-i)\ \Gamma A_2)}{\det(M)^2} \\ &= i\ \frac{\mathrm{Tr}(M^{-1}\ \Gamma A_2)}{\det(M)}, \end{aligned}$$

and then one obtains:

$$\Im(\partial_t \varphi(s,0)) = \Re\left(\frac{\mathrm{Tr}(M_{t=0}^{-1}\ \Gamma A_2)}{\det(M_{t=0})}\right),$$

which concludes the proof.

Acknowledgement

This research was supported by the French ANR TIPHAINE (ANR-25-CE48-3360).

References

[1] P. Flandrin, "Time–frequency filtering based on spectrogram zeros," *IEEE Signal Processing Letters*, vol. 22, no. 11, pp. 2137–2141, 2015.

[2] R. Bardenet, J. Flamant, and P. Chainais, "On the zeros of the spectrogram of white noise," *Applied and Computational Harmonic Analysis*, vol. 48, no. 2, pp. 682–705, 2020.

[3] L. D. Abreu, A. Haimi, G. Koliander, and J. L. Romero, "Filtering with wavelet zeros and Gaussian analytic functions," *arXiv preprint arXiv:1807.03183*, 2018.

[4] J. B. Hough, M. Krishnapur, Y. Peres *et al.*, *Zeros of Gaussian analytic functions and determinantal point processes*. American Mathematical Soc., 2009, vol. 51.

[5] R. Bardenet and A. Hardy, "Time-frequency transforms of white noises and gaussian analytic functions," *Applied and computational harmonic analysis*, vol. 50, pp. 73–104, 2021.

[6] J. Xiao and P. Flandrin, "Multitaper time-frequency reassignment for nonstationary spectrum estimation and chirp enhancement," *IEEE Transactions on Signal Processing*, vol. 55, no. 6, pp. 2851–2860, 2007.

[7] I. Daubechies, Y. G. Wang, and H.-T. Wu, "Conceft: Concentration of frequency and time via a multitapered synchrosqueezed transform," *Philosophical transactions. Series A, Mathematical, physical, and engineering sciences*, vol. 374, no. 2065, p. 20150193, 2016.

[8] K. Gröchenig and Y. Lyubarskii, "Gabor frames with hermite functions," *Comptes Rendus Mathematique*, vol. 344, no. 3, pp. 157–162, 2007.

[9] ——, "Gabor (super) frames with hermite functions," *Mathematische Annalen*, vol. 345, no. 2, pp. 267–286, 2009.

[10] M. Faulhuber, I. Shafkulovska, and I. Zlotnikov, "Asymptotic safety regions for gabor frames generated by hermite functions," *arXiv preprint arXiv:2609.01296*, 2026.

[11] L. D. Abreu and T. Shirai, "Zero correlations and averaged fields of orthonormal gaussian functions," *arXiv preprint arXiv:2605.17296*, 2026.

[12] A. Haimi, G. Koliander, and J. L. Romero, "Zeros of gaussian weyl–heisenberg functions and hyperuniformity of charge," *Journal of Statistical Physics*, vol. 187, no. 3, p. 22, 2022.

[13] K. Gröchenig, *Foundations of time-frequency analysis*. Springer, 2001, vol. 359.

[14] L. D. Abreu, "On the structure of Gabor and super Gabor spaces," *Monatshefte für Mathematik*, vol. 161, no. 3, pp. 237–253, 2010.

[15] V. Bargmann, "On a Hilbert space of analytic functions and an associated integral transform," *Communications on pure and applied mathematics*, vol. 14, no. 3, pp. 187–214, 1961.

[16] L. D. Abreu and H. G. Feichtinger, "Function spaces of polyanalytic functions," in *Harmonic and complex analysis and its applications*. Springer, 2013, pp. 1–38.

[17] L. D. Abreu, "Sampling and interpolation in bargmann–fock spaces of polyanalytic functions," *Applied and Computational Harmonic Analysis*, vol. 29, no. 3, pp. 287–302, 2010.

[18] D. Armentano, J.-M. Azaïs, and J. R. León, "On a general kac–rice formula for the measure of a level set," *The Annals of Applied Probability*, vol. 35, no. 3, pp. 1828–1851, 2025.

[19] G. L. Turin, "The characteristic function of hermitian quadratic forms in complex normal variables," *Biometrika*, vol. 47, no. 1/2, pp. 199–201, 1960.

[20] O. Sète and J. Zur, "On the zeros of polyanalytic polynomials," *Journal of Mathematical Analysis and Applications*, vol. 540, no. 1, p. 128595, 2024.

[21] A. Haimi, G. Koliander, and J. L. Romero, "Phasejumps: fast computation of zeros from planar grid samples," *arXiv preprint arXiv:2603.13158*, 2026.

[22] W. Rudin, *Principles of mathematical analysis*, 3rd ed. McGraw-Hill, 2021.

[23] ——, *Real and complex analysis*. McGraw-Hill, 1974.

[24] V. Jacquemet, "Phase singularity detection through phase map interpolation: theory, advantages and limitations," *Computers in biology and medicine*, vol. 102, pp. 381–389, 2018.

[25] L. Isserlis, "On a formula for the product-moment coefficient of any order of a normal frequency distribution in any number of variables," *Biometrika*, vol. 12, no. 1/2, pp. 134–139, 1918.

[26] G. Casella and R. Berger, *Statistical inference*. CRC press, 2024.